Journal of Polymers and the Environment
https://doi.org/10.1007/s10924-024-03308-3

ORIGINAL PAPER

Evaluation of Anti-Biofilm and in Vitro Wound Healing Activity of Bacterial Cellulose Loaded with Nanoparticles and Borax

Nur Bozbeyoglu Kart[1] · Mine Sulak[2] · Doğukan Mutlu[3] · Volkan Kuzucu[3] · Sevki Arslan[3] · Nazime Mercan Dogan[3]

Accepted: 30 April 2024

Abstract

Biofilms are a severe problem for public health because of the contributing recurrence of infections. Therefore, combating biofilms is a critical issue. In our study, we loaded zinc oxide (ZnO), zinc oxide borax (ZnOBorax), zinc copper oxide ($ZnCuO_2$) nanoparticles and borax into bacterial cellulose (BC) to impart anti-biofilm and wound healing activity. The prepared BC loaded with nanoparticles (BC–NPs) was analysed via scanning electron microscopy. The nanoparticles' geometric structure and placement in BC fibres were observed. We evaluated the biofilm inhibition and biofilm degradation activities of the BC–NPs against some pathogens via a crystal violet (CV) assay and XTT (2,3-bis(2-methoxy-4-nitro-5-sulfophenyl)-2 H-tetrazolium-5-carboxanilide) reduction assay. The effects of BC–NPs on cell proliferation and wound-healing ability were analysed in L929 cell line. BC–NPs exhibited better biofilm degradation activity than biofilm inhibition activity. According to the results of the CV assay, BC–ZnONPs, BC–Borax and BC–ZnOBoraxNPs inhibited 65.53%, 71.74% and 66.60% of biofilm formation of *Staphylococcus aureus*, respectively. BC–$ZnCuO_2$NPs showed the most degradation activity on *Pseudomonas aeruginosa* and *Listeria innocua* biofilms. The XTT reduction assay results indicated a considerable reduction in the metabolic activity of the biofilms. Moreover, compared to the control group, BC loaded with borax and ZnO nanoparticle promoted cell migration without cytotoxicity.

Keywords Bacterial cellulose · Nanoparticle · Modification · Anti-biofilm · Wound healing

Introduction

Bacterial cellulose (BC) is an ideal polymer for many applications in biomedical fields due to its non-toxic effect, high water retention capacity, biocompatibility and easy shaping properties [1–4]. Moreover, its characteristic properties are important in antimicrobial agents and anti-cancer treatments. However, unmodified BC has been restricted for therapeutic applications [4]. Therefore, BC needs to be modified to increase its biological properties as a biomedical material. Many studies have modified BC. For example, Fernandes et al. (2013) modified antimicrobial BC membranes by adding amino alkyl groups [5]. In other studies, BC nanoribbons were partially acetylated by catalysation with citric acid or hydrolysed using different acid concentrations (H_2SO_4 and HCl) and reaction times for nanocrystal formation [6, 7]. Some researchers have modified BC by changing its surface charge using carboxyl groups [8]. Hyaluronic acid–BC composites, chitosan–BC composites, cactus/BC hydrogels and metallic nanoparticles combined with BC have also been obtained by numerous researchers to improve the biological properties of BC [9–11]. Moreover, researchers have reported that BC composites with pullulan, chitosan, cactus and acrylic acid hydrogels increase the healing rate of burn wounds and may be used as wound dressing composites [11–15]. In addition, BC for skin wound treatment have antimicrobial efficacy. In this regard, antimicrobial peptides with quorum quenching enzymes, silver nanoparticles, zinc oxide nanoparticles, and carbon quantum dots–titanium dioxide (CQD–TiO_2) nanoparticles

✉ Nazime Mercan Dogan
nmercan@pau.edu.tr

1 Department of Plant and Animal Production, Tavas Vocational High School, Pamukkale University, Denizli, Turkey

2 Faculty of Applied Sciences, Department of Organic Agricultural Management, Pamukkale University, Denizli, Turkey

3 Faculty of Science, Department of Biology, Pamukkale University, Denizli, Turkey

Published online: 20 June 2024

have been used to impart antibacterial and antimicrobial properties to BC [16–19]. Biofilm, produced by pathogenic bacteria, is a complex community of microbes adhering to natural or synthetic structures and firmly embedded in the extracellular matrix [20]. Pathogenic bacteria in biofilms exchange genetic material with each other, and the genetic modifications in pathogens cause them to develop resistance to antibiotics. Currently, antibiotic resistance has led to an increase in infectious diseases and epidemics. Additionally, biofilms play an essential role in the infection processes of pathogens. For example, the presence of biofilms in chronic wounds is one of the factors that impair the healing process [21, 22]. Therefore, there is a need for materials that can penetrate and disrupt bacterial biofilms in the health sector. Modified BC can also be used to prevent biofilm formation, which is a structure that increases the pathogenicity of bacteria and causes many treatments to fail in the clinic [23]. In this regard, BC nanoparticles inhibit bacterial biofilm production, which is also being produced due to the anti-biofilm effects of nanoparticles, such as Ag, Zn and boron [24]. These BC nanoparticles could serve as important biomedical materials, especially in wound dressing applications or to minimise biofilm growth. Some researchers have determined the antibacterial activities of metal oxide nanoparticles, such as zinc oxide, copper oxide [25, 26] and boron [27, 28]. While these nanoparticles and boron show specific toxic properties on bacteria, they have little effect on human cells (25–28).

As previously mentioned, metal oxide (ZnO and CuO) nanoparticles and borax may be alternatives for limiting bacterial biofilm formation. According to the literature, antimicrobial agents, such as boron, silver, copper and zinc, have been incorporated to endow BC with antibacterial efficacy [19, 28–33]. Still, the anti-biofilm activities of synthesised composites have yet to be reported. CuO and ZnO nanoparticles are nanoparticles that have many applications such as sensors, biomedical and antibacterial. In addition, the mentioned nanoparticles were preferred due to easy to obtain by green synthesis method, cheap and harmless to nature [25, 32]. Thus, we aimed to develop BC loaded with nanoparticles (BC-NPs) with anti-biofilm efficacy. BC formed from *Gluconobacter xylinus* S4 isolate was loaded with zinc oxide nanoparticles (ZnONPs), borax and a combination (ZnOBoraxNPs and $ZnCuO_2$NPs). The BC-NPs were analysed to determine their physicochemical properties by scanning electron microscopy (SEM). Moreover, we study their anti-biofilm, cytotoxic, and wound-healing properties.

Materials and Methods

Preparation of BC Loaded with Nanoparticles (BC-NPs)

Copper oxide nanoparticles (CuONPs) and zinc oxide nanoparticles (ZnONPs) used in the experiment were synthesised by the green synthesis method [34]. Borax pentahydrate (analytical grade) was purchased from Merck. Composites prepared with BC were synthesised *ex situ* [1]. After that, four BCs (4×4 cm plates) were placed in 200 mL of water that contain either ZnONPs (0.1 g), borax (0.1 g), ZnOBoraxNPs (0.05 g ZnONPs and 0.05 g borax) or $ZnCuO_2$NPs (0.05 g ZnONPs and 0.05 g CuONPs). Then, they were agitated at 200 rpm at 50 °C for 48 h. The synthesised four different BC-NPs were dried and stored for analysis [35].

Analysis of the BC Loaded with Nanoparticles (BC-NPs) by SEM

The morphologies and elemental compositions of the BC-NPs were investigated by SEM (using a scanning electron microscope, Zeiss Supra 40 VP, Oberkochen, Germany) and energy dispersive X-ray spectroscopy (EDX), respectively. The samples were sputter-coated with gold–palladium particles (Quorum Q150R ES, Quorum Technologies Ltd, Lewes, UK), and the accelerator voltage was adjusted to 30 kV.

Determination of Biofilm Inhibition and Biofilm Degradation Activity of BC-NPs

Crystal Violet (CV) Assay

The activities of biofilm inhibition and degradation of the BC–NPs were determined via the CV assay method [36, 37]. In this study, we used *Listeria innocua* ATCC 33090, *Staphylococcus aureus* ATCC 29213, *Pseudomonas aeruginosa* PAO1, *Escherichia coli* ATCC 10536, *Streptococcus parasanguinis* ATCC 15909, *Bacillus cereus* RSKK 863, *Enterococcus hirae* ATCC 10541 and *Candida albicans* ATCC 64548 as human pathogens. Sabouraud Dextrose Broth (SDB, for *Candida albicans*), Todd Hewitt Broth (for *Streptococcus* strains) and Tryptic Soya Broth (for other bacteria) were used as growth media. Each cell culture (10% microbial inoculum/medium, 0.5 MacFarland) was added to wells containing the growth medium with BC–NPs (as sheet) and incubated at 37°C for 48 h to determine the biofilm inhibition activity. Then, the samples were removed from the wells and the wells were washed with PBS (0.01 M, pH 7.4) to remove non-adherent cells. Each well in

the plate was stained with 0.1% CV for 15 min. Then, 33% glacial acetic acid for gram-positive bacteria and *Candida albicans* and 95% ethanol for gram-negative bacteria were added to the wells. The optical density of the wells was read at 570 nm in a microtitre plate spectrophotometer (Epoch, Biotech). All tests were performed in duplicate. The formula below was used to determine the activity percentage of the BC–NPs.

Anti-biofilm activity (%) = [(Control OD – Sample OD) / Control OD] × 100.

To determine the biofilm degradation efficacy of the BC–NPs, microbial biofilms were grown at 48 h, and then, non-adherent cells were removed by washing with PBS. The BC–NPs were added to each well, and the plates were incubated at 24 h. Finally, the biofilm degradation was determined using the above method [38].

XTT Assay

The viability of each microbial strains in the biofilm was evaluated via the XTT assay [39–42]. After incubation for 48 h, the plates were washed with phosphate-buffered saline (PBS, 0.01 M, pH 7.2). Then, 100 µL of PBS and 50 µL of XTT reaction solution were loaded (Cell Proliferation Kit (XTT-based), Biological Industries, Israel). Then, the plates were incubated in a dark room at 37 °C for 5 h. Absorbance was measured at 450–630 nm. To determine the biofilm degradation effect of the BC–NPs, we added them to the wells containing pre-formed biofilms and incubated them for 12 and 24 h. At the end of the incubation period, all BC–NPs were removed, and each well was gently washed three times with PBS. A standard XTT reduction assay was performed to quantify the viability of the biofilm via bacterial metabolic activity. The decrease in metabolic activity compared to the control biofilm formed (100%) in the wells without BC–NPs is defined as the biofilm inhibition and degradation effect. The experiments involved two replicates. The formula below was used to determine the activity percentage of the BC–NPs.

Anti-biofilm activity (%) = 100- [(Sample OD / Control OD) × 100]

Cell Culture and Treatment

Mouse fibroblast cell lines (L929) are typically used as model cells in biocompatibility studies of biomaterials [43]. The L929 cell line was purchased from the American Type Culture Collection (ATCC). It was grown in Dulbecco's Modified Eagle's Medium (DMEM, Sigma) and enriched with 10% heat-inactivated foetal bovine serum (FBS, Capricorn) and 1% penicillin/streptomycin solution (100X, Capricorn), as described previously [44]. The cells were cultured in a 100-mm cell culture dish (Nest) and incubated at 37 °C and 5% CO_2 in a humidified CO_2 incubator. The viability of the L929 cells was examined using MTT (3-(4, 5-dimethylthiazol2-yl)-2, 5-diphenyl tetrazolium bromide) reagent (Merck), as previously described [45]. For this, cells were harvested with 0.25% Trypsin-EDTA (Capricorn) at 90% confluence and seeded at a density of 2×10^3 cells/well in a 96-well plate (Costar, Corning) in a complete medium. After 24 h, the medium was replaced with different concentrations (25, 50 and 100%) of the medium containing BC–NPs. For the extraction, The BC–NPs sheets were sterilised by autoclaving at 121 °C for 15 min and placed on a six-well plate. The extraction conditions were based on ISO 10993-12 as described previously with slight modifications [1]. Briefly, 2 × 3 cm cut BC–NPs sheets (6 cm^2/mL) was extracted at 37 °C for 24 h in culture media in a shaker. After 24 h, the medium was removed and filtered. An equal amount of fresh medium was added to untreated cells (negative control). After incubation period of the cells with BC-NPs (24 h) culture medium was removed, and 10 µL of MTT (5 mg/mL) was added to each well and incubated under culture conditions. Cell viability was calculated as decribed previsouly [45].

In Vitro Cell Migration Assay

The migration efficacy of BC–NPs was evaluated using the wound healing assay described previously [46]. In this study, the L929 mouse fibroblast cell line was selected. Fibroblast cells have been proposed to test wound healing capacity in *in-vitro* studies [47]. Briefly, 3×10^4 cells were plated into 6-well plates (Jet Biofil) and incubated under culture conditions. After 24 h, the cells were scraped with a 200-µL pipette tip [48] and washed with phosphate-buffered saline (PBS, Bioshop) to discard detached cells. The medium containing the non-toxic concentrations of BC–NPs was replaced for 24 h. The wound area in the treated cells was compared with the vehicle group. The wound size was captured (0, 24, 48 and 72 h) using an inverted microscope (Oxion Inverso, Euromex) at 10× magnification, and the wound closure rate (%) was analysed using ImageJ software 1.53e, as described previously [49].

Statistical Analysis

GraphPad Prism 9 (San Diego, CA, USA) was used for statistical analysis. The experiments were performed in triplicate, and the data are expressed as means ± SD. Two-way ANOVA was used to analyse the statistical differences between the groups. Ns = not significant, * = $p < 0.05$, ** = $p < 0.005$, *** = $p < 0005$, **** = $p < 0.0001$.

Results and Discussion

Bacterial Cellulose Loaded with Nanoparticles

As shown in Fig. 1, the morphology of BC loaded with nanoparticles was determined via SEM analysis. As shown in the electron microscope images, the nanoparticles on BC generally had an oval geometry. The nanoparticles likely penetrated deeply into the BC fibre networks. In other words, we speculated that nanoparticles bind strongly to BC fibrils owing to the hydroxyl groups in the chemical structure of native BC. This positively affects many biological properties of BC. Moreover, the quantitative analysis of BC modified with nanoparticles is shown in Fig. 1. Eventually, strong peaks in the EDX spectrum showed the formation of BC–NPs.

Determination of Biofilm Inhibition and Biofilm Degradation

Biofilms in chronic wounds delay their healing [50]. This is because the biofilm-forming feature of pathogens increases their infectivity and makes it difficult to combat them. Moreover, the bacteria in the biofilm structure escape the host defence more easily. For example, *P. aeruginosa* biofilm delayed wound healing compared to a group without the biofilm because of its prolonged inflammatory phase of healing [51]. Because antibiotics cannot penetrate the biofilm structure, the pathogens in a biofilm are almost always protected from the effects of drugs. Therefore, bacterial biofilms are a significant problem for human health. In our previous paper, the pure BC membrane did not exhibit any anti-biofilm activity, showing that non-modified BC did not have anti-biofilm activity against tested strains in the study, except *S. aureus* with a biofilm inhibition percentage of 22% [1]. However, BC–NP research is a recently developing field due to nanoparticles' strong antimicrobial and anti-biofilm activities. In this study, we evaluated BC–NPs and their biofilm inhibition effect, biofilm degradation, and metabolic activity of microorganisms in the biofilm structure. Various human pathogenic microorganisms were used, and the activities of biofilm inhibition and degradation of BC–NPs were screened using a CV assay. According to the CV staining results, the effects on the biofilm growth and the development of a preformed biofilm were different (Table 1). It has been reported that different antimicrobial activities against different bacteria could lead to different extents of biofilm inhibition by nanoparticles [52]. In this study, the *S. aureus* ATCC 29213 biofilm was reduced by 65.53% by BC–ZnONPs, 71.74% by BC–BoraxNPs, 66.60% by BC–ZnOBoraxNPs and 28.27% by BC–ZnOCuO_2NPs. Of the four BC–NPs, BC–BoraxNPs showed the highest effect on *S. aureus* ATCC 29213, followed by BC–ZnOBorax and BC–ZNONPs. The lowest biofilm inhibition effect was observed with BC–ZnOCuO_2NPs (Table 1). The biofilm inhibition against *P. aeruginosa* PAO1 could not be observed for all BC–NPs, whereas BC–ZnONPs and BC–Borax had moderate inhibitory potential with 38.44 and 39.97% on *E. coli* ATCC 10536, respectively. The BC–NPs showed a more potent inhibitory capacity against *S. aureus* than *E. coli* and *P. aeruginosa* because the cell wall structure of gram-negative cells is more sophisticated than the cell structure of gram-positive cells that have a more substantial defence capability [53, 54]. BC–ZnONPs, BC–Borax and BC–ZnCuO_2NPs inhibited the biofilm formation of *L. innocua* ATCC 33090 at 44.79, 54.86 and 65.14%, respectively. BC–Borax showed the highest biofilm inhibition activity at 57.12% in *C. albicans* ATCC 64548 as a eukaryotic microorganism. The biofilm inhibition effect of BC–NPs was lower on other tested bacteria, as shown in Table 1. BC loaded with Zn$OCuO_2$ nanoparticles did not show any effect on both degradation and inhibition of *P. aeruginosa* PA01, *S. parasanguinis* ATCC 15909, *B. cereus* RSKK 863, *E. hirae* ATCC 10541 and *C. albicans* ATCC 64548 biofilms. In comparing the 24-h biofilm degradation, BC–Borax was the most effective at reducing *P. aeruginosa* PAO1, *L. innocua* ATCC 33090 and *S. parasanguinis* ATCC 15909 biofilms by 58.98, 62.40 and 54.26%, respectively, BC–ZnOBoraxNPs degraded 64.02% (for *S. aureus* ATCC 29213) and 52.93% (for *L. innocua* ATCC 33090) of the bacterial biofilm. According to the CV assay, the biofilm degradation of BC–NPs was likely related to the biofilm degrading ability of ZnO, borax, and CuO. However, other BC–NPs had no significant degradation effect on the pre-biofilm. Borax and nanoparticles, such as ZnO and CuO, have been reported to have inhibitory effects on bacterial biofilm formation [28, 32, 55].

To evaluate the biofilm inhibition and eradication activities of the BC–NPs by using the XTT reduction assay, we selected *L. innocua* ATCC 33090, *S. aureus* ATCC 29213, *P. aeruginosa* PAO1, *E. coli* ATCC 10536, *S. parasanguinis* ATCC 15909 and *C. albicans* ATCC 64548. The anti-biofilm efficacy of BC–NPs was further confirmed by measuring the metabolic activity of the cells in the biofilm. The results obtained from the CV assay were not correlated with the XTT reduction assay. In other words, the biofilm inhibition of BC–ZnCuO_2NPs was determined by the XTT reduction assay despite no biofilm inhibition shown in the CV assay. Moreover, the biofilm inhibition activity of BC–ZnCuO_2NPs had the highest effects against *C. albicans* ATCC 64548, *S. aureus* ATCC 29213, *L. innocua* ATCC 33090 and *E. coli* ATCC 10536. Moreover, there was no significant inhibition effect for ZnONPs, Borax, and ZnOBoraxNPs against the tested microorganisms. The metabolic activities

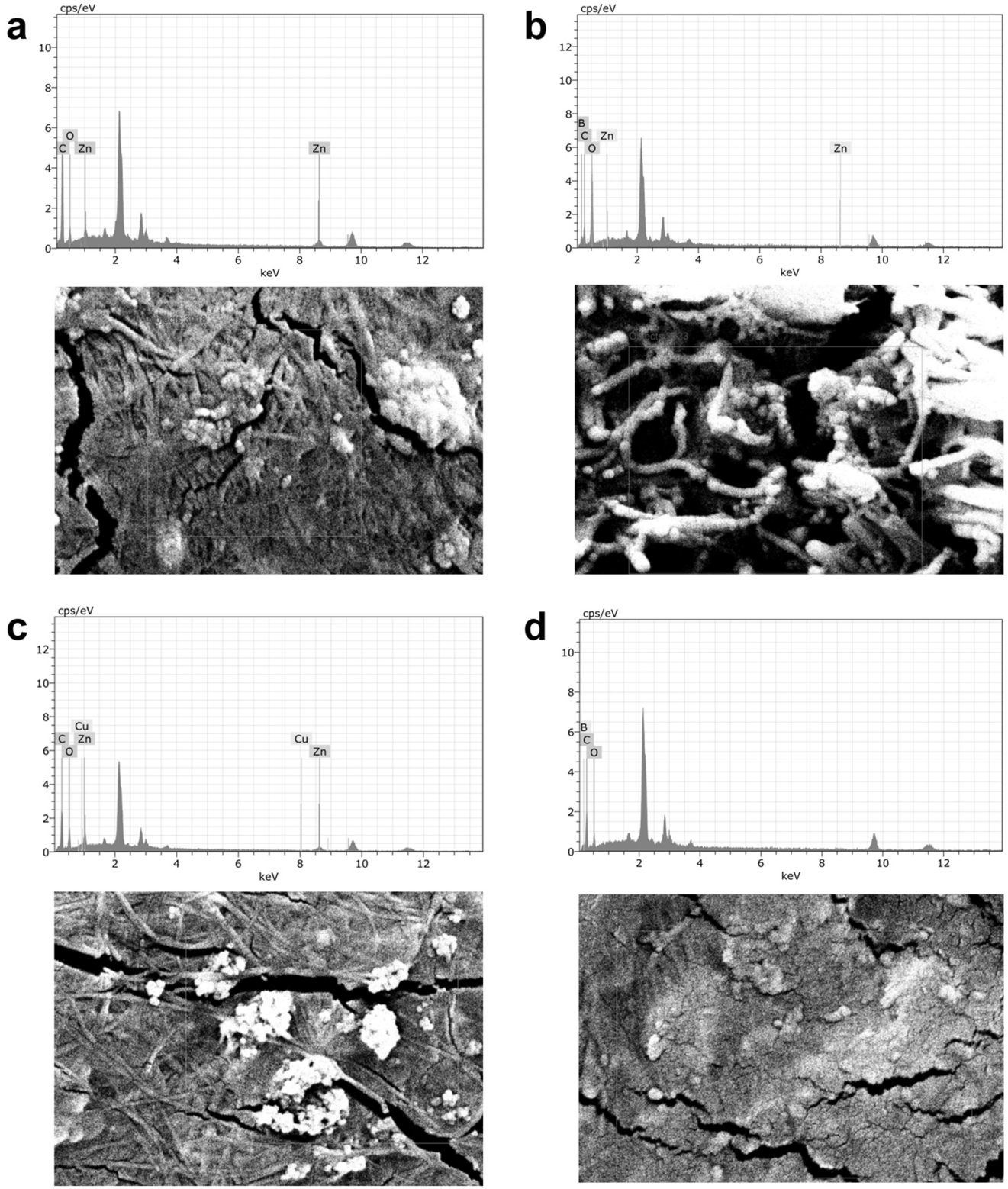

Fig. 1 Scanning electron microscopy (SEM) images at 50.00 kx magnification and energy dispersive X-ray spectrum of BC and the nanohybrids. **a, b, c** and **d** show ZnO, ZnOBorax, $ZnCuO_2$ nanoparticles (NPs) and Borax, respectively

Table 1 Biofilm inhibition percentages and degradation results from the CV assay (%)

	ZnO		Borax		ZnOBorax		$ZnOCuO_2$	
	Inhibition	Degradation	Inhibition	Degradation	Inhibition	Degradation	Inhibition	Degradation
Escherichia coli ATCC 10536	$38.44 \pm 0.00^{**}$	$35.47 \pm 3.71^{**}$	$39.97 \pm 0.00^{**}$	$39.41 \pm 5.43^{**}$	$11.35 \pm 3.01^{*}$	$37.52 \pm 8.08^{**}$	19.57 ± 4.58^{ns}	21.47 ± 6.94^{ns}
Pseudomonas aeruginosa PA01	$5.55 \pm 0.00^{**}$	$48.99 \pm 0.00^{**}$	-	$58.98 \pm 5.83^{**}$	-	$18.42 \pm 0.00^{**}$	-	-
Staphylococcus aureus ATCC 29213	$65.53 \pm 0.00^{**}$	-	$71.74 \pm 0.19^{**}$	$29.91 \pm 1.76^{**}$	$66.60 \pm 4.15^{*}$	$64.02 \pm 0.44^{**}$	-	28.27 ± 4.93^{ns}
Listeria innocua (6a) ATCC 33090	$44.79 \pm 1.34^{**}$	$53.43 \pm 4.97^{**}$	$54.86 \pm 7.38^{**}$	$62.40 \pm 0.62^{**}$	$11.61 \pm 0.00^{*}$	$52.93 \pm 5.72^{**}$	65.14 ± 0.60^{ns}	39.4 ± 1.75^{ns}
Streptococcus parasanguinis ATCC 15909	-	$28.82 \pm 0.00^{**}$	$26.22 \pm 0.00^{**}$	$54.26 \pm 0.75^{**}$	$2.83 \pm 0.00^{*}$	$26.94 \pm 0.50^{**}$	-	-
Bacillus cereus RSKK 863	$14.55 \pm 0.00^{**}$	-	$10.83 \pm 0.00^{**}$	-	$37.73 \pm 6.75^{*}$	-	-	-
Enterococcus hirae ATCC 10541	$29.23 \pm 0.00^{**}$	$11.33 \pm 0.00^{**}$	$34.78 \pm 7.94^{**}$	$43.43 \pm 0.00^{**}$	$18.97 \pm 2.05^{*}$	$34.34 \pm 1.68^{**}$	-	-
Candida albicans ATCC 64548	$38.41 \pm 0.00^{**}$	$27.93 \pm 9.92^{**}$	$57.12 \pm 2.28^{**}$	$12.21 \pm 0.00^{**}$	$23.75 \pm 0.00^{*}$	$22.90 \pm 0.00^{**}$	-	-

-: Not determined, ns: not significant, $^{*}p < 0.05$, $^{**}p < 0.005$

of these cells continued in the presence of nanoparticles. During bacterial biofilm formation, the most resistant bacteria to nanoparticles were *P. aeruginosa* PAO1 and *S. parasanguinis* ATCC 15909. In other words, these bacteria continued their metabolic activities in the presence of BC–NPs. There was no inhibition in bacterial biofilm formation (Fig. 2). However, we still chose to test the degradation effect of BC–NPs due to the effects of these bacteria on public health. However, there was no inhibition against these two bacteria. Interestingly, BC–NPs were observed to have degradation abilities against the biofilm formed by these bacteria (Fig. 3).

According to the results, the biofilm degradation efficacy of BC–NPs upon treatment for 24 h was higher than with treatment for 12 h (Fig. 3). Moreover, the biofilm degradation percentage increased, indicating the degradation effectivity of some BC–NPs against pathogens. In particular, while all BC–NPs showed high degradation activity against *S. parasanguinis* ATCC 15909 at 24 h (BC–ZnONPs: 85.49 ± 3.24%, BC–Borax: 69.09 ± 0.00%, BC–ZnOBoraxNPs: 59.70 ± 0.00% and BC–$ZnCuO_2$NPs: 69.04 ± 8.58%) (Fig. 4d), only BC–ZnOBoraxNPs (52.10 ± 1.84%) showed moderate degradation sensitivity at 12 h (Fig. 3b). For *P. aeruginosa* PAO1, BC–ZnONPs (77.21 ± 3.91%) and BC–Borax (76.40 ± 1.05%) showed a similar degradation percentage at 12 h. Still, this effect of BC–ZnONPs and BC–Borax decreased at 24 h. BC–$ZnCuO_2$NPs interestingly degraded 87.740.61 ± 0.00% of the *P. aeruginosa* PAO1 biofilm in 24 h (Fig. 3c). Similarly, BC–$ZnCuO_2$NPs induced degradation of the biofilm against *L. innocua* ATCC 33090 by up to 87.72 ± 4.03% in 24 h (Fig. 3c). Moreover, a decrease in the metabolic activity of cells of the biofilm was observed with the BC–NPs. Not all BC–NPs showed degradation activity against *C. albicans* ATCC 64548 with high levels of metabolic activity (Fig. 3c and d).

Our modified BC–NPs showed degradation of the bacterial biofilm. Similarly, BC loaded with chitosan nanoparticles showed biofilm eradication activities (36.09–90.43%) against pre-existing bacterial biofilms [21]. According to Zhang and co-authors, a BC + tannic acid + Mg composite showed a strong antibacterial effect against *S. aureus*, *E. coli* and *P. aeruginosa* bacteria and reduced biofilm formation of *S. aureus* (80%), and *P. aeruginosa* (87%) [56]. Moreover, a BC + chitosan nanocomposite showed antimicrobial activity against *S. aureus, P. aeruginosa* and *C. albicans* and prevented biofilm formation on the nanocomposite surfaces [57]. Furthermore, our results indicated that the anti-biofilm activity of BC–NPs was related to the variety of nanoparticles and tested microorganisms. Previous studies indicated that nanoparticles, such as copper, zinc, and borax, had been used to inhibit biofilm formation [28, 58,

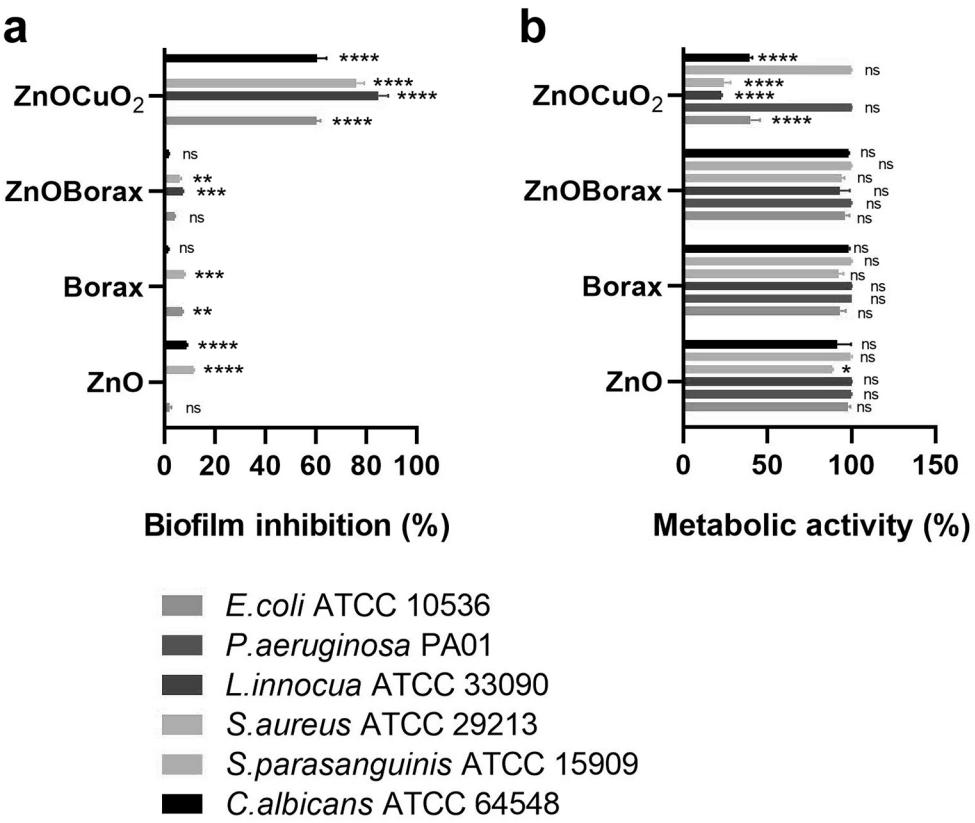

Fig. 2 Biofilm inhibition percentages of BC–NPs (**a**) and metabolic activities of the cells in the biofilm (**b**) compared to the control. The results shown are the means ± SD. Ns = not significant, * = $p < 0.05$, ** = $p < 0.005$, *** = $p < 0005$, **** = $p < 0.0001$

59]. In our study, the reduction in biofilm formation after treatment with BC–NPs may be related to the anti-biofilm effect of possibly damaging the cell membrane after the interaction of the nanoparticles with the bacteria or damaging bacterial DNA, as Brahma and co-authors mentioned [60]. The mechanism of biofilm degradation is unclear. However, the rapid destruction of the biofilm may also be related to the interruption of bacterial cell signalling systems and degradation of the biofilm matrix [61]. Moreover, the biofilm inhibition and degradation results may be due to the differences in microorganism strains and the effect of nanoparticles in the BC modification. Finally, as expected, decreases in metabolic activity were noted where the anti-biofilm effect was high.

MTT Assay

The in vitro compatibility of BC–NPs was determined on mouse fibroblast L929 cells by MTT assay. Three different concentrations of BC–NPs (25, 50 and 100%) were applied for cytocompatibility investigations for 24 h. Results from the MTT assay of the BC–NPs showed no significant effects on the cell viability at a concentration of 25% (Fig. 4). We did not observe any cytotoxic effect due to BC itself. We observed a cytotoxic effect as the concentration increased due to the nanoparticles remaining in the nutrient substitute. We also observed a cytotoxic effect as the concentration increased due to the nanoparticles remaining in the culture medium. Therefore, the highest non-cytotoxic doses of nanoparticles were selected for further studies.

Wound Healing Assay

A wound healing assay was performed to assess the effects of BC loaded with ZnONPs, ZnOBoraxNPs, Borax and $ZnCuO_2$NPs (highest non-cytotoxic concentrations of 25, 50, 50 and 25%, respectively) on the migration of L929 cells (Fig. 5). Following 24 h of treatment, the medium containing BC–NPs was removed from individual wells, the cells were washed with PBS twice, and the medium was refreshed. Note that the control group contained only culture medium.

BC and its different composites are considered suitable biomaterials for tissue engineering and regenerative medicine, especially for their significant contribution to wound healing [62–64]. Czaja et al. (2006) suggested that the unique nanofibrillar structure of BC–based wound dressings contributes to their biocompatibility by providing an ideal environment for wound healing [65]. BC accelerates skin healing compared to traditional wound dressings, such as ointments and wet gauze [66, 67]. Research has shown that

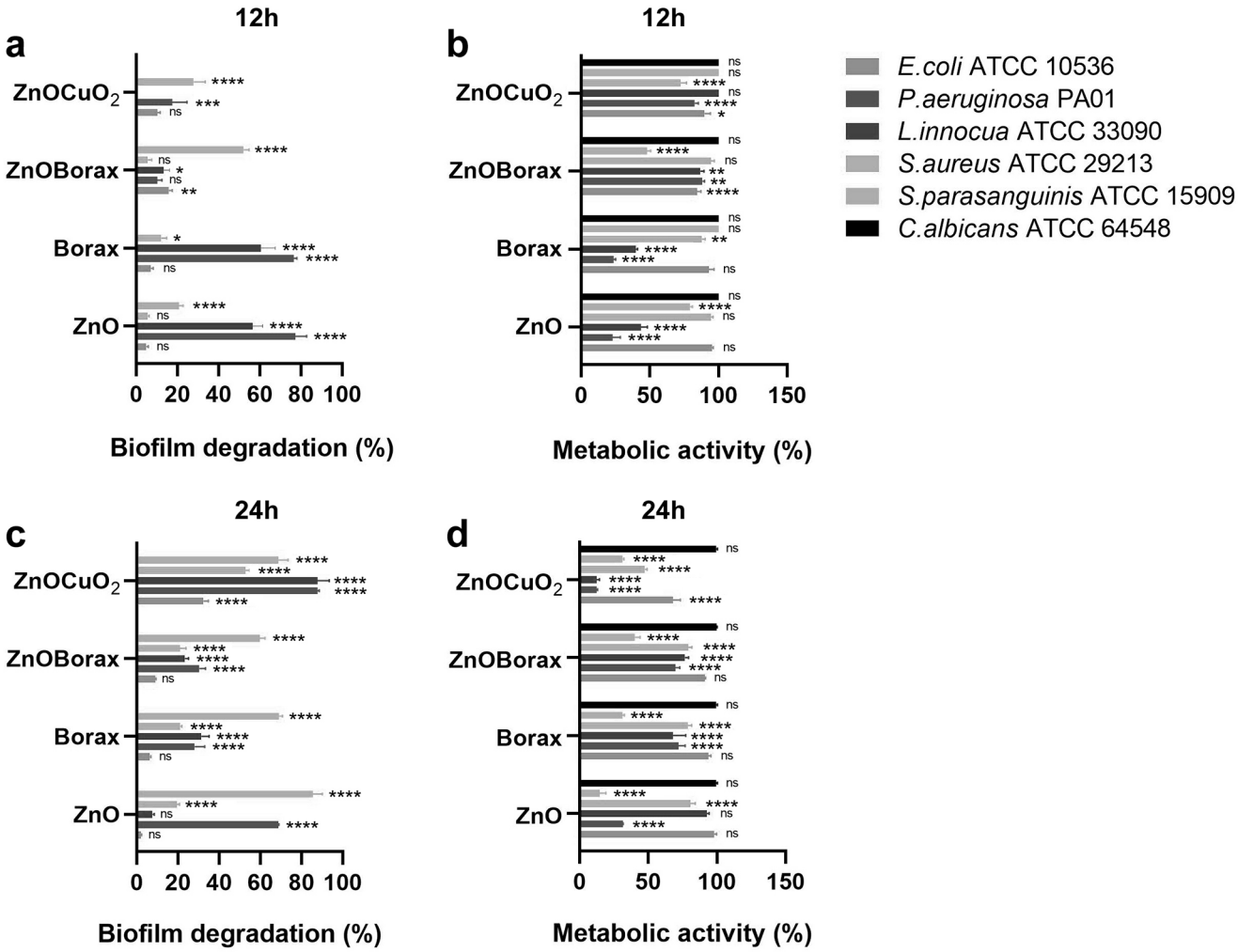

Fig. 3 Biofilm degradation and metabolic activity of cells with BC–NPs in the biofilm structure compared to the control. The results shown are means ± SD. Ns = not significant, * = $p < 0.05$, ** = $p < 0.005$, *** = $p < 0.0005$, **** = $p < 0.0001$

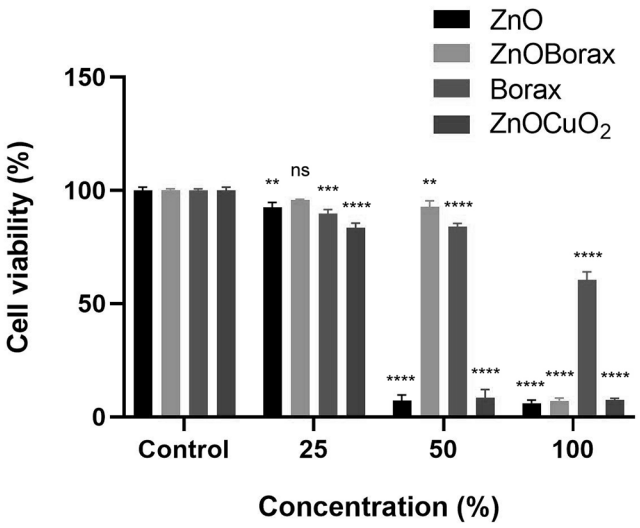

Fig. 4 Cytocompatibility of BC extracts on L929 mouse fibroblast cells for 24 h. The results are shown as means ± SD. Ns = not significant, ** = $p < 0.005$, *** = $p < 0005$, **** = $p < 0.0001$

BC–based coverings lower rates of wound infection and accelerate re-epithelization [65, 68, 69].

In our study, the migration of L929 cells was significantly induced by BC–Borax, and cell migration reached 99% (Fig. 6). The wound area in the BC–ZnONPs (5.2%) was better than in the control group (6.4%) at 72 h. However, the wound area of cells treated with ZnOBoraxNPs and $ZnCuO_2$NPs was found to be 18.5 and 22.3%, respectively, after 72 h. In other words, cell migration was restricted approximately three- and four-fold compared to the control cells in the same order. Similar to our findings, BC nanocomposites containing different nanoparticles showed wound-healing properties in prior studies [63, 70–72]. It is well established that zinc oxide nanoparticles have many properties, including wound healing by changing cell migration, re-epithelialization, and angiogenesis [73]. Similarly, BC has wound-healing activity due to its unique properties, including a uniform nanofiber network, high crystallinity, high

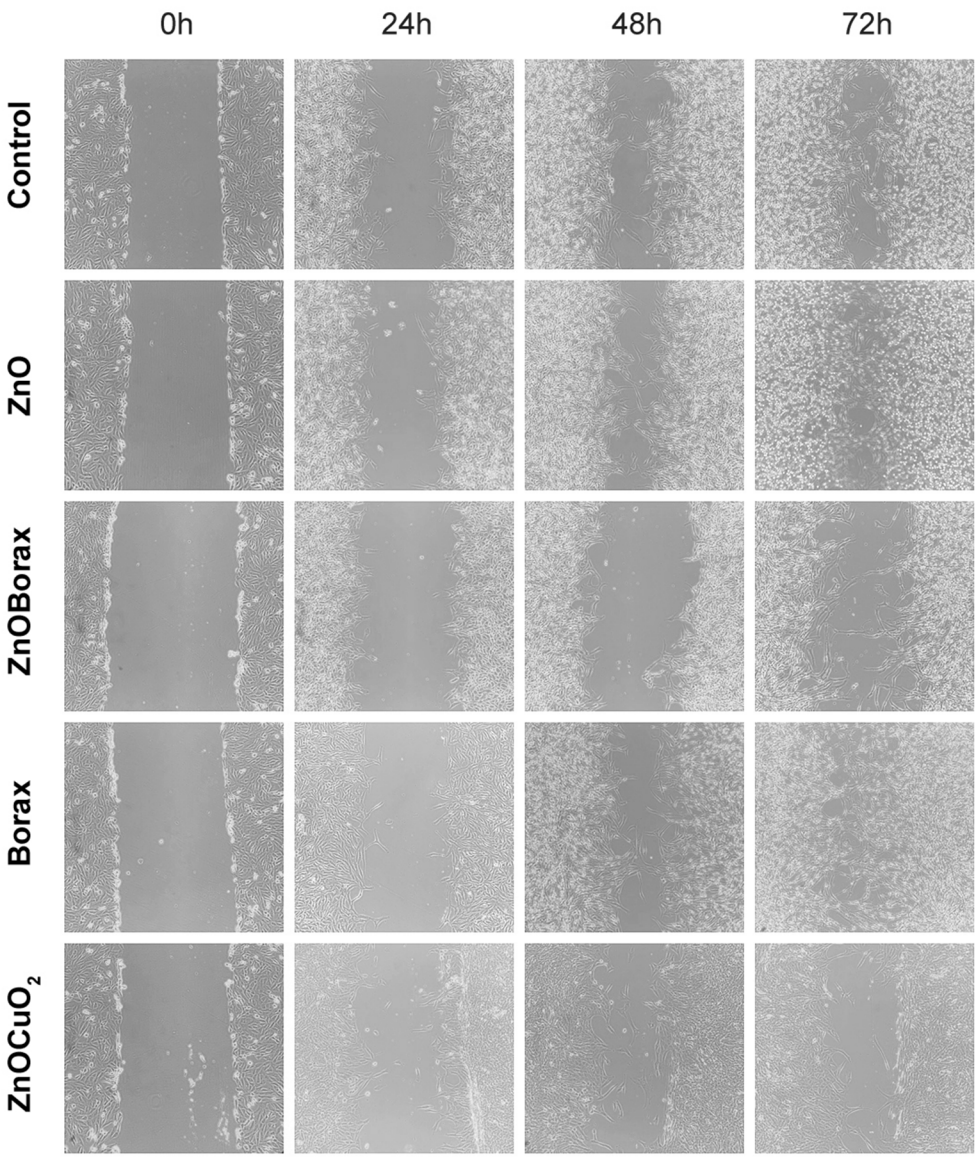

Fig. 5 Microscope images from the in vitro wound healing assay of BC extracts. The photos were taken at 0, 24, 48, and 72 h

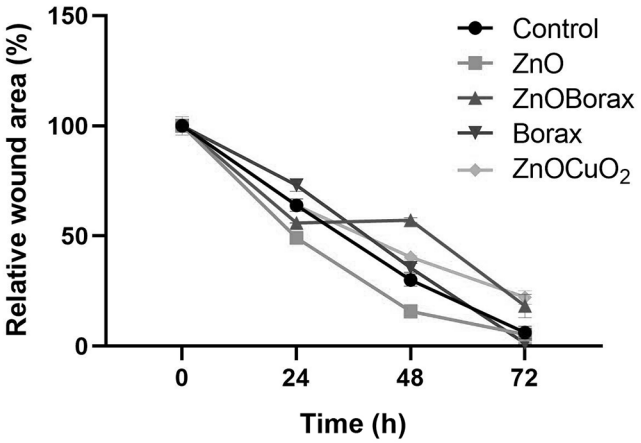

Fig. 6 Percentage of wound area for treated cells compared to the control at 0, 24, 48, and 72 h. The data shown are the means ± SD. Control group wound areas were taken to be 100% and calculated using ImageJ software

water absorption, and retention capacity [74]. Moreover, borax loading could increase wound healing activity [75]. In this regard, BC–ZnO and BC–Borax showed better wound-healing properties. Additionally, our results showed for the first time that BC–Borax has potential wound-healing activity for L929 fibroblast cells.

Conclusion

In the present study, BC was successfully modified with ZnONPs, borax, ZnOBoraxNPs and $ZnCuO_2$NPs, and they were confirmed by SEM analysis. The BC- $ZnCuO_2$NPs showed good antibiofilm activity against *C. albicans* ATCC 64548, *E. coli* ATCC 10536, *S. aureus* ATCC 29213 and *L. innocua*. Moreover, the biofilm degradation efficacy of

BC–ZnONPs, BC–Borax, and BC–$ZnCuO_2$NPs towards preformed biofilms of *P. aeruginosa* and *L. innocua* were significant. Also, BC–Borax and BC–ZnONPs have showed wound healing activity. All of these results suggest that BC-NPs can be considered for use in wound-healing dressings and other biomedical applications by restricting and inhibiting biofilm formation towards different bacteria in wounds.

Author Contributions N.M.D. contributed the direction of experimental studies, evaluation of results, supply of resources and materials and wrote the article; M.S. modified BC with nanoparticles and borax, V.K., N.B.K. and D.M. performed the experiments, creation of figures and table; D.M. and S.A. evaluated the results of wound healing and cytotoxic activity. All authors checked the final file of article.

Funding Open access funding provided by the Scientific and Technological Research Council of Türkiye (TÜBİTAK).

Data Availability No datasets were generated or analysed during the current study.

Declarations

Competing interests The authors declare that there are no conflicts of interest.

References

1. Top B et al (2021) Production and characterization of bacterial cellulose from *Komagataeibacter Xylinus* isolated from home-made Turkish wine vinegar. Cellul Chem Technol 55(3–4):243–254
2. Kalyani P, Khandelwal M (2021) Modulation of morphology, water uptake/retention, and rheological properties by in-situ modification of bacterial cellulose with the addition of biopolymers. Cellulose 28:11025–11036
3. Hou Y et al (2018) Development and biocompatibility evaluation of biodegradable bacterial cellulose as a novel peripheral nerve scaffold. J Biomed Mater Res A 106(5):1288–1298
4. Munair B et al (2021) Properties and Applications of modified bacterial cellulose-based materials. Curr Nanosci 17(3):351–364
5. Fernandes SC et al (2013) Bioinspired antimicrobial and biocompatible bacterial cellulose membranes obtained by surface functionalization with aminoalkyl groups. ACS Appl Mater Interfaces 5(8):3290–3297
6. Ávila Ramírez JA et al (2016) Acetylation of bacterial cellulose catalyzed by citric acid: use of reaction conditions for tailoring the esterification extent. Carbohydr Polym 153:686–695
7. Vasconcelos NF et al (2017) Bacterial cellulose nanocrystals produced under different hydrolysis conditions: Properties and morphological features. Carbohydr Polym 155:425–431
8. Wu CN et al (2018) TEMPO-Oxidized bacterial cellulose pellicle with silver nanoparticles for Wound Dressing. Biomacromolecules 19(2):544–554
9. Lopes TD et al (2014) Bacterial cellulose and hyaluronic acid hybrid membranes: production and characterization. Int J Biol Macromol 67:401–408
10. Khamrai M, Banerjee SL, Kundu PP (2017) Modified bacterial cellulose based self-healable polyeloctrolyte film for wound dressing application. Carbohydr Polym 174:580–590
11. Kamal T et al (2022) Preparation, characterization, and Biological features of Cactus Coated Bacterial Cellulose Hydrogels. Gels 8(2):88
12. Atila D et al (2022) Pullulan hydrogel-immobilized bacterial cellulose membranes with dual-release of vitamin C and E for wound dressing applications. Int J Biol Macromol 218:760–774
13. Mohamad N et al (2019) In vivo evaluation of bacterial cellulose/acrylic acid wound dressing hydrogel containing keratinocytes and fibroblasts for burn wounds. Drug Deliv Transl Res 9(2):444–452
14. Stanescu PO et al (2021) Novel chitosan and bacterial cellulose biocomposites tailored with polymeric nanoparticles for modern wound dressing development. Drug Deliv 28(1):1932–1950
15. Prasathkumar M, Sadhasivam S (2021) Chitosan/Hyaluronic acid/Alginate and an assorted polymers loaded with honey, plant, and marine compounds for progressive wound healing-know-how. Int J Biol Macromol 86:656–685
16. Aslanli A et al (2020) Bacterial cellulose containing combinations of antimicrobial peptides with various QQ enzymes as a prototype of an enhanced Antibacterial Dressing: in Silico and in Vitro Data. Pharmaceutics 12(12):1155
17. Malmir S et al (2020) Antibacterial properties of a bacterial cellulose CQD-TiO2 nanocomposite. Carbohydr Polym 234:115835
18. Mocanu A et al (2019) Bacterial cellulose films with ZnO nanoparticles and propolis extracts: synergistic antimicrobial effect. Sci Rep 9(1):17687
19. Barud HS et al (2011) Antimicrobial bacterial cellulose-silver nanoparticles Composite membranes. J Nanomaterials 2011: Article ID 721631:8
20. Roy R et al (2018) Strategies for combating bacterial biofilms: a focus on anti-biofilm agents and their mechanisms of action. Virulance 9:522–554
21. Zmejkoski DZ et al (2021) Chronic wound dressings – pathogenic bacteria anti-biofilm treatment with bacterial cellulose-chitosan polymer or bacterial cellulose-chitosan dots composite hydrogels. Int J Biol Macromol 191:315–323
22. Salisbury AM et al (2018) Tolerance of biofilms to antimicrobials and significance to antibiotic resistance in wounds. Surg Technol Int 33:59–66
23. Soumya S et al (2016) Review on bacterial biofilm: an universal cause of contamination. Biocatal Agric Biotechnol 7:56–66
24. Hasanzadeh A et al (2023) Biosynthesis of MCC/IL/Ag-AgCl NPs by cellulose-based Nanocomposite for Medical Antibiofilm Applications. Ind Eng Chem Res 62(11):4729–4737
25. Doğan SŞ, Kocabaş A (2020) Green synthesis of ZnO nanoparticles with Veronica Multifida and their antibiofilm activity. Hum Exp Toxicol 39(3):319–327
26. Khalaji AD et al (2020) CuO nanoparticles: preparation, characterization, optical properties, and antibacterial activities. J Mater Sci: Mater Electron 31:11949–11954

27. Sayin Z, Ucan US, Sakmanoglu A (2016) Antibacterial and Antibiofilm effects of Boron on different Bacteria. Biol Trace Elem Res 173:241–246
28. Kıvanç M et al (2018) Effects of hexagonal boron nitride nanoparticles on antimicrobial and antibiofilm activities, cell viability. Mater Sci Eng C Mater Biol Appl 91:115–124
29. Luiz CS et al (2010) Preparation and Antibacterial Activity of Silver Nanoparticles Impregnated in Bacterial Cellulose. Polímeros: Ciência e Tecnologia 20(3):72–77
30. He W et al (2018) In situ synthesis of bacterial cellulose/copper nanoparticles composite membranes with long-term antibacterial property. J Biomater Sci Polym Ed 29(17):2137–2153
31. Ma B et al (2016) Novel Cu@SiO2/bacterial cellulose nanofibers: Preparation and excellent performance in antibacterial activity. Mater Sci Eng C Mater Biol Appl 62:656–661
32. Mohamed AA et al (2021) Eco-friendly mycogenic synthesis of ZnO and CuO nanoparticles for in Vitro Antibacterial, Antibiofilm, and antifungal applications. Biol Trace Elem Res 199(7):2788–2799
33. Kai J, Xuesong Z (2020) Preparation, characterization, and cytotoxicity evaluation of Zinc Oxide–Bacterial cellulose–chitosan hydrogels for Antibacterial Dressing. Macromol Chem Phys 221:2000257
34. Sulak M (2021) Preparation of G-CuO NPs and G-ZnO NPs with mallow leaves, investigation of their antibacterial behavior and synthesis of bis(indolyl)methane compounds under solvent-free microwave-assisted dry milling conditions using G-CuO NPs as a catalyst. Turk J Chem 45:1517–1532
35. Jebel SF, Almasi H (2016) Morphological, physical, antimicrobial and release properties of ZnO nanoparticles-loaded bacterial cellulose films. Carbohydr Polym 149:8–19
36. Nostro A et al (2016) In vitro activity of plant extracts against biofilm-producing food-related bacteria. Int J Food Microbiol 238:33–39
37. Leathers TD et al (2018) Inhibition of *Streptococcus mutans* and *S. sobrinus* biofilms by liamocins from *Aureobasidium pullulans*. Biotechnol Rep 21:e00300
38. Sahin C et al (2021) New iridium bis-terpyridine complexes: synthesis, characterization, antibiofilm and anticancer potentials. Biometals 34:701–713
39. Adukwu E, Allen SC, Phillips CA (2012) The anti-biofilm activity of lemongrass (Cymbopogon flexuosus) and grapefruit (Citrus paradisi) essential oils against five strains of *Staphylococcus aureus*. J Appl Microbiol 113:1217–1227
40. Subramenium GA, Vijayakumar K, Pandian SK (2015) Limonene inhibits streptococcal biofilm formation by targeting surface-associated virulence factors. J Med Microbiol 64:879–890
41. Sivaranjani M et al (2016) Morin inhibits biofilm production and reduces the virulence of *Listeria monocytogenes*—An in vitro and in vivo approach. Int J Food Microbiol 237:73–8234
42. Xu Z et al (2016) Crystal Violet and XTT assays on *Staphylococcus aureus* Biofilm quantification. Curr Microbiol 73:474–482
43. Zange R, Kissel T (1997) Comparative in vitro biocompatibility testing of polycyanoacrylates and poly(d,l-lactide-co-glycolide) using different mouse fibroblast (L929) biocompatibility test models. Eur J Pharm Biopharm 44(2):149–157
44. Sen A et al (2015) Modulatory actions of o-coumaric acid on carcinogen-activating cytochrome P450 isozymes and the potential for drug interactions in human hepatocarcinoma cells. Pharm Biol 53(9):1391–1398
45. Konus M et al (2022) Synthesis and biological activity of new indole based derivatives as potent anticancer, antioxidant and antimicrobial agents. J Mol Struct 1263:133168
46. Yılmaz C et al (2021) Identification of 3-Bromo-1-Ethyl-1H-Indole as a potent Anticancer Agent with Promising Inhibitory effects on GST isozymes. Anticancer Agents Med Chem 21(10):1292–1300
47. Abe Y et al (2000) Wound healing acceleration of a novel transforming growth factor-beta inducer, SEK-1005. Eur J Pharmacol 408(2):213–218
48. Qazi TH et al (2017) Biomaterials that promote cell-cell interactions enhance the paracrine function of MSCs. Biomaterials 140:103–114
49. Suarez-Arnedo A et al (2020) An image J plugin for the high throughput image analysis of in vitro scratch wound healing assays. PLoS ONE 15(7):e0232565
50. Gajula B et al (2020) How bacterial biofilms affect chronic wound healing: a narrative review. Int J Surgery: Global Health 3:e16
51. Zhao G et al (2010) Delayed wound healing in diabetic (db/db) mice with Pseudomonas aeruginosa biofilm challenge: a model for the study of chronic wounds. Wound Repair Regen 18(5):467–477
52. Palanisamy NK et al (2014) Antibiofilm properties of chemically synthesized silver nanoparticles found against *Pseudomonas aeruginosa*. J Nanobiotechnol 12:2
53. Cai M et al (2022) Antibacterial and antibiofilm activities of chitosan nanoparticles loaded with *Ocimum basilicum* L. essential oil. Int J Biol Macromol 202:122–129
54. Vahedikia N et al (2019) Biodegradable zein film composites reinforced with chitosan nanoparticles and cinnamon essential oil: physical, mechanical, structural and antimicrobial attributes. Colloids Surf B: Biointerfaces 17:25–32
55. Akhil K et al (2016) Effect of various capping agents on photocatalytic, antibacterial and antibiofilm activities of ZnO nanoparticles. J Photochem Photobiol B 160:32–42
56. Zhang ZY et al (2020) A biocompatible bacterial cellulose/tannic acid composite with antibacterial and anti-biofilm activities for biomedical applications. Mater Sci Eng C 106:110249
57. Cabañas-Romero VL et al (2020) Bacterial cellulose–Chitosan Paper with Antimicrobial and antioxidant activities. Biomacromolecules 21(4):1568–1577
58. Shehabeldine AM et al (2023) Potential antimicrobial and Antibiofilm properties of Copper Oxide nanoparticles: Time-kill kinetic essay and ultrastructure of pathogenic bacterial cells. Appl Biochem Biotechnol 195(1):467–485
59. Khan F et al (2020) Antibiofilm Action of ZnO, SnO2 and CeO2 nanoparticles towards Grampositive Biofilm forming pathogenic Bacteria. Recent Pat Nanotechnol 14(3):239–249
60. Brahma U et al (2018) Antimicrobial and anti-biofilm activity of hexadentated macrocyclic complex of copper (II) derived from thiosemicarbazide against *Staphylococcus aureus*. Sci Rep 8:8050
61. Yasir M et al (2018) Action of antimicrobial peptides against bacterial biofilms. Materials 11:2468:1–15. https://doi.org/10.3390/ma11122468
62. Ossowicz-rupniewska P et al (2021) Transdermal delivery systems for ibuprofen and ibuprofen modified with amino acids alkyl esters based on bacterial cellulose. Int J Mol Sci 22:6252
63. Melnikova N et al (2021) Wound Healing Composite materials of bacterial cellulose and zinc oxide nanoparticles with immobilized Betulin Diphosphate. Nanomaterials 11(3):713
64. He W et al (2022) Bacterial cellulose/soybean protein isolate composites with promoted inflammation inhibition, angiogenesis and hair follicle regeneration for wound healing. Int J Biol Macromol 211:754–766
65. Czaja W et al (2006) Microbial cellulose the natural power to heal wounds. Biomaterials 27:145–151
66. Fu L, Zhang J, Yang G (2013) Present status and applications of bacterial cellulose-based materials for skin tissue repair. Carbohydr Polym 92:1432–1442

67. Ahmed J, Gultekinoglu M, Edirisinghe M (2020) Bacterial cellulose micro-nano fibres for wound healing applications. Biotechnol Adv 41:107549
68. Fink H et al (2010) Real-time measurements of coagulation on bacterial cellulose and conventional vascular graft materials. Acta Biomater 6:1125–1130
69. Rajwade JM, Paknikar KM, Kumbhar JV (2015) Applications of bacterial cellulose and its composites in biomedicine. Appl Microbiol Biotechnol 99:2491–2511
70. Khalid A et al (2017) Bacterial cellulose-zinc oxide nanocomposites as a novel dressing system for burn wounds. Carbohydr Polym 164:214–221
71. Isopencu G et al (2023) Bacterial cellulose-carboxymethylcellulose composite loaded with Turmeric Extract for Antimicrobial Wound dressing applications. Int J Mol Sci 24(2):1719
72. He W et al (2023) Fabrication of Cu2+-loaded phase-transited lysozyme nanofilm on bacterial cellulose: Antibacterial, anti-inflammatory, and pro-angiogenesis for bacteria-infected wound healing. Carbohydr Polym 309:120681
73. Khan AUR et al (2021) Exploration of the antibacterial and wound healing potential of a PLGA/silk fibroin based Electrospun membrane loaded with zinc oxide nanoparticles. J Mater Chem B 9(5):1452–1465
74. He W et al (2021) Bacterial cellulose: functional modification and Wound Healing Applications. Adv Wound Care (New Rochelle) 10(11):623–640
75. Tantiwatcharothai S, Prachayawarakorn J (2020) Property improvement of antibacterial wound dressing from basil seed (*O. Basilicum* L.) mucilage- ZnO nanocomposite by borax crosslinking. Carbohydr Polym 227:115360